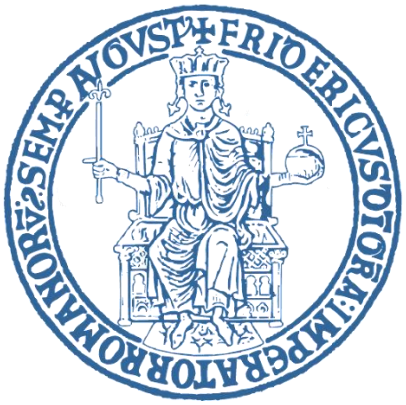

Università degli Studi di Napoli "Federico II"

SCUOLA POLITECNICA E DELLE SCIENZE DI BASE DIPARTIMENTO DI INGEGNERIA INDUSTRIALE

CORSO DI LAUREA IN INGEGNERIA AEROSPAZIALE CLASSE DELLE LAUREE IN INGEGNERIA INDUSTRIALE (L-9)

BACHELOR THESIS

PRELIMINARY SIZING AND FLIGHT PERFORMANCE OF A TWIN-ELECTRIC POWERED RC AIRCRAFT

Main flight maneuvers

Candidate: **MATTEO MANGONE**
Matricola: **N35002493**

Supervisor	**Co-Supervisor**
Dr. DANILO CILIBERTI	Prof. Eng. FABRIZIO NICOLOSI

Word count: 9000 academic year 2020/2021

Abstract

The following paper will delve into the design process of an aircraft model aimed to observe the guidelines of the *Design Build and Fly* competition from 2019.

In the first two chapters, the reader will be presented with the general procedure that leads to the selection of the specific final configuration for the aircraft, which is the result of a parametrical conceptual design process based on logical observations backed up with aerodynamics and aircraft performances know-how.

Once the design is selected, a series of iterations regarding weight examination, based on empirical data, provides the reader with the final estimated weight of the aircraft, fundamental for the final phase of the research, concerning flight performances.

The last chapter analyses the twin-engine configuration of the aircraft, which refers to the placement of each engine on a dedicated pylon on top of the wing structure. The choice of the twin-engine, which splits the power requirement between the two brushless motors, will have a considerable impact on the performances and weight of the aircraft compared to the single-engine configuration, which data are already available.

The analysis aims to study the effect of the split power source on the main maneuvers that the aircraft is expected to perform in the course of the competition, those being takeoff, climb, cruise and landing. To those, a further gliding analysis is added to anticipate the behavior of the aircraft in the unfortunate case of a powertrain fail.

The results, paired with the previous analysis, have helped further understand the advantages and disadvantages of adopting either a single or twin-engine configuration for lightweight aircraft models.

Table of contents

0 Indexes

0.0 List of figures

0.1 List of Tables

0.2 Abbreviations

- TO – Take-off
- LG – Landing gear
- TD – Touch-down
- AoA – Angle of attack
- SR – Sink rate
- RC – Radio-controlled

The reader will find it useful to consult the previous index each time he is faced with abbreviations meant to ease the flow of the discussion.

1 Chapter 1 - Introduction

1.0 Team Organization

The team appointed to the realization of the model is a subgroup of the team formed in 2019 to participate in the Design Build and Fly (DBF) competition that would have been held the following year. The missions and requirements taken into consideration have been established starting from the ones of the competition. This project has given each member of the team the opportunity to improve several soft skills such as team working and problem-solving which are relevant and decisive for an engineer. In addition, this experience has allowed the team to deepen its knowledge in the Aerospace Engineering field, providing the fundamentals of aircraft design in the context of an experimental bachelor's thesis.

The team counts five members to better focus each one's work on the five branches identified that will lead to the final design of the aircraft, called by the team as "UninAir". Consequently, every member of the team is the leader of their own branch and therefore its manager. The team has been supervised by two advisors that proved guidance to the team throughout the whole project. The identified branches concern: the study of the aerodynamics of the aircraft through the use of software such as AIRFOIL and XFLR5; examination of the stability of the model with the aid of the program created by NASA, OpenVSP; structural analysis, in particular, an accurate check was performed on the wing structure, in presence of aerodynamic loads; aircraft performance analysis (polar curves, propeller performance). It is clear that each branch is not isolated from the others, but there is a strong link between all the application fields considered and therefore a coordinated work by each member of the Team is required.

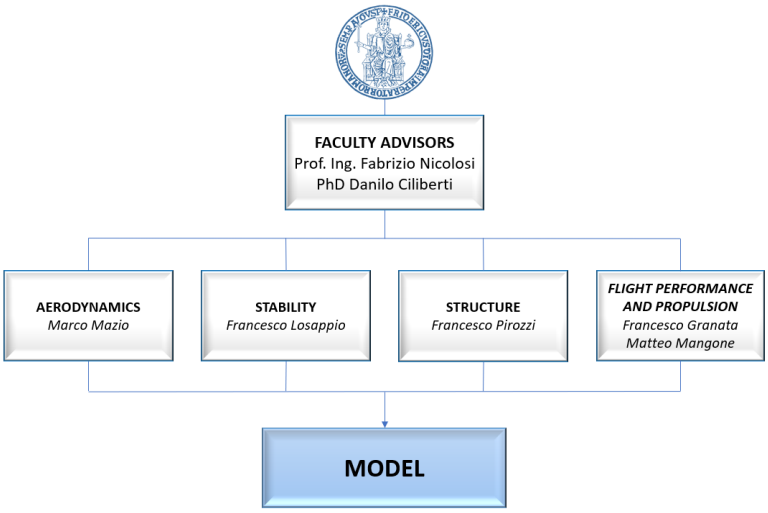

Figure 1-1. Team organization

1.0.1 Requirements

The main purpose of the team was to carry as many passengers as possible, in order to allow the aircraft to score the most points. In the table below, there is an overview of the requirements that the team had to take into account during the project:

Maximum allowable wingspan	$5\ ft = 1.5\ m$
Take-Off Gross Weight with payload	$TOGW < 55\ lb = 25\ kg$
Passenger Weight	$5\ oz = 113.4\ g$
Luggage Weight	$1\ oz = 28.35\ g$
Take-Off Run	$23\ ft = 7\ m$
Ground for the take-off	$Dirt$
Endurance	$10\ min$
Minimum load for bending test	$\pm\ 3x\ MTOW$
Type of Propulsion	$Electric$

Table 1-1. Requirements of the competition

In addition, the aircraft has to follow the path shown in Figure 1-2, and each lap must be completed in 2 minutes or less, as lap time is also one of the parameters subjected to the scoring process.

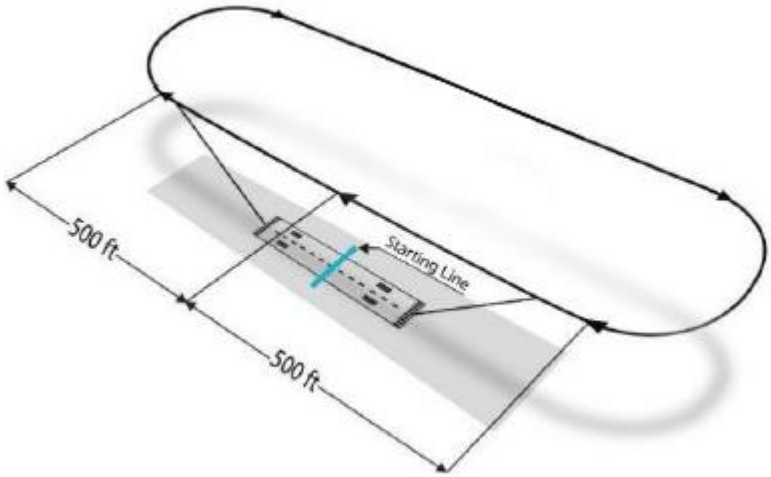

Figure 1-2. Competition path

The dimension of each passenger and luggage are defined in the figures below:

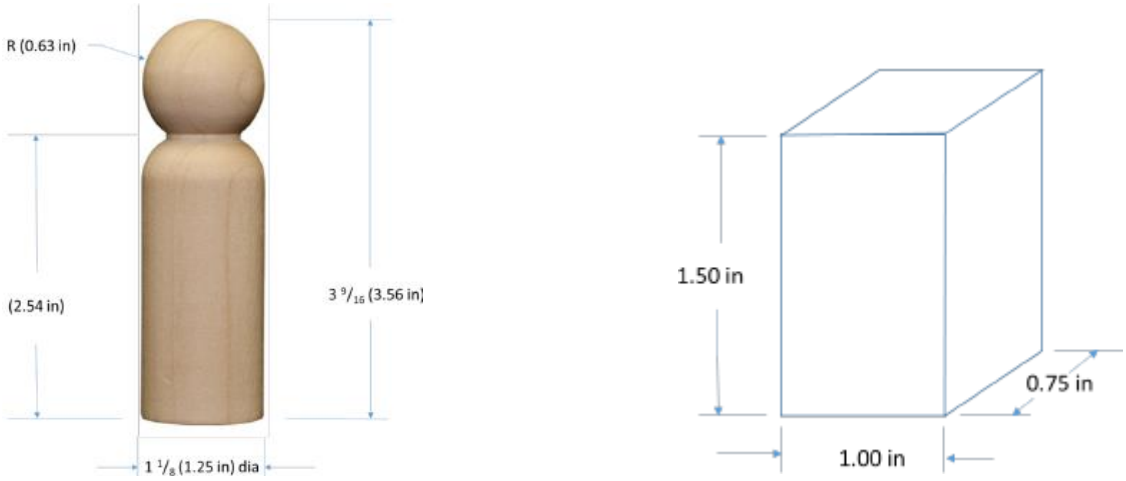

Figure 1-3. Passenger dimensions

2 Chapter 2 - Preliminary Design and Sizing

2.0 Design selection process

To properly choose the best configuration for the aircraft, the team has compiled a table of merit based on the most important configuration factors. It has been assigned a score from 0 to 5 for each one, depending on the mission requirements.

Factor	Importance
Structural Weight	4
Maneuverability	3
Passengers Capability	5
Speed	3,5
Manufacturability	4,5
Take-OFF Run	2,5
Reliability	2,5

Table 2-1. Factors' index of importance

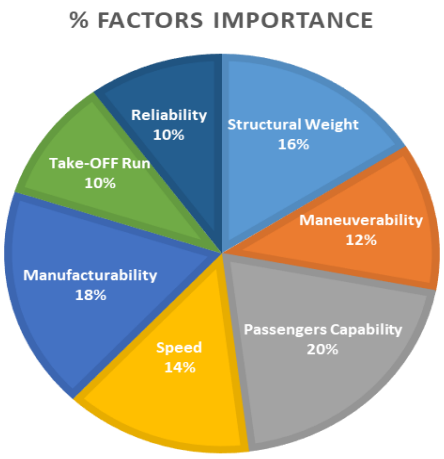

Figure 2-1. Factors importance

- **Structural Weight**: the weight strongly influences the performance of the aircraft. Lower structural weight means either less consumption or more payload transportable.
- **Maneuverability**: the capability to safely control the aircraft, as well as its stability, are important to complete all the laps on time.
- **Passengers Capability**: this is the most important factor because carrying as many passengers as possible would provide more points.
- **Speed**: the airplane speed contributes to complete faster the mission, although a trade-off study is necessary to avoid excessive consumption of the batteries.
- **Manufacturability**: the ease of manufacturing is essential since building the aircraft will be up to the team. Therefore, some configurations have been rejected due to complex manufacturing and lack of experience in those processes.
- **Take-Off Run**: having a short take-off run is included among the requirements. This forced the team to take into account configurations that would provide advantages on those terms.
- **Reliability**: to guarantee safety during the missions (take-off, cruise, and landing), the reliability of the aircraft is not a negligible factor.

Feature	Configuration	Wing	Tailplane	Engine	Landing Gear	Fuselage
Result	CONVENTIONAL	LOW	CONVENTIONAL	SINGLE/TWIN	TRICYCLE	RECTANGULAR

Table 2-2. Final design decision

The final conceptual design has been chosen by analyzing the total score gained by each different configuration in terms of Structural Weight, Maneuverability, Passenger Capability, Speed, Manufacturability, Take-off Run, and Reliability as shown so far. The total score is obtained by adding up scores assigned to each possible configuration as it will be shown further in this document.

2.1 Conceptual Design

Considering the requirements of the mission, it is appropriate to present the layout of the team's arguments regarding how the bulk of the design was figured out. As a general note, the focus was on:

- **Main wing configuration**
- **Main wing positioning**
- **Tail section**
- **Engines**
- **Landing gear**
- **Fuselage**

This preliminary discussion is crucial to further analyze the capabilities of the aircraft, the choice made in those regards will form the foundations of the specialized studies that aim to reach the optimal configuration.

Component	Alternatives		
Wing Layout	Conventional	Biplane	Flying Wing
Wing Positioning	Low	High	
Empennage Type	V-Tail	Conventional	T-Tail
Number of Engines	1	2	
Landing Gear	Taildragger	Tricycle	
Fuselage section	Smoothed Rectangular	Circular	

Table 2-3. Design Alternatives

2.1.1 Main Wing Configuration

The choice of the main wing configuration of the aircraft is the first aspect on which attention has been focused upon. That is because it is important to adapt the subsequent decisions regarding the individual components of the aircraft to this primary one.
The observed configurations are:

- CONVENTIONAL: it is composed of the tailplane (horizontal and vertical) and one main wing.

- BIPLANE: two overlapping wings which are parallel to each other although they may have different shapes and sizes.
- FLYING WING: flying wing aircrafts without fuselage and tailplane.

From a structural weight's point of view, the best one is the flying wing since it is the lightest, because of the tailplane absence. However, the flying wing does not excel on directional stability due to the absence of the fin and this directly affects maneuverability. It's important to point out that the flying wing configuration will have high longitudinal stability if equipped with reflex airfoil (self-stable) and if the warping factors and the sweep angle are well evaluated.

Regarding the biplane it must be said that with the same wingspan of a conventional configuration there is twice as much wing area, halving the wing load. Moreover, the eventual presence of a double aileron implies a higher roll rate and therefore more lateral maneuverability.

Focusing on reliability, the conventional configuration is the best known of the three considered and therefore well proven to be dependable. The biplane is frequently subject to assembly inaccuracies since it is the most complex.

Both the biplane and flying wing models are very difficult to manufacture since they require unconventional construction techniques.

The flying wing is the one that generates less drag among the three. On the other hand, the biplane configuration, with the presence of two main lift generators, create four vortexes that massively increase aerodynamic drag. The conventional is a good compromise between the previous two.

Regarding the passengers' capacity, the biplane is the most inconvenient because it is difficult to create a passage for the insertion of passengers due to the presence of wing braces between the two wings.

Biplane configuration has a lower take-off length since, with the same wingspan, the wing surface is double, and therefore the wing load decreases. The opposite situation occurs with the flying wing, also because of the lack of flaps.

CONFIGURATION TRADE STUDY							
		CONVENTIONAL		FLYING WING		BIPLANE	
Attribute	Weighting	Insert Score	Weighted score	Insert Score	Weighted score	Insert Score	Weighted score
Structural Weight	16%	0.6	0.096	1	0.16	0.3	0.048
Maneuverability	12%	0.8	0.096	0.5	0.06	0.6	0.039
Passengers Capability	20%	0.8	0.16	0.3	0.06	0.7	0.081
Speed	14%	0.8	0.112	1	0.14	0.4	0.037
Manufacturability	18%	1	0.18	0.25	0.045	0.5	0.065
Take-OFF Run	10%	0.9	0.09	0.7	0.07	1	0.083
Reliability	10%	1	0.1	0.5	0.05	0.6	0.055
Total	100%		0.83		0.59		0.41

Table 2-4. Configuration trading study

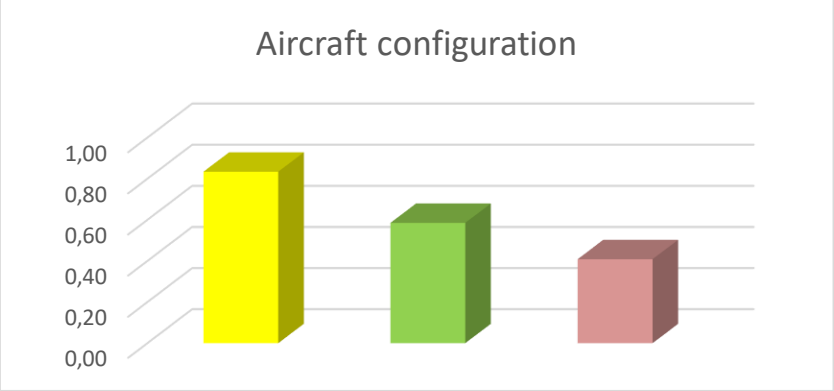

Figure 2-2. Configuration Trade Study

2.1.2 Wing Positioning

Once opted for the conventional configuration for our aircraft, two different wing positions have been taken into consideration: high wing and low wing. As is shown in the table below, the passenger capacity is the parameter that most influenced our choice.

In terms of structural weight, the low wing configuration is slightly better because it allows embedding the spar in the force frames. This is not possible with a high wing that should be installed on the upper surface of the fuselage, where the access point is supposed to be located. However, in case of a braced wing, the root sections could be slenderer because in that zone the momentum is null.

An aircraft with a high wing has a better (static) lateral stability thanks to the dihedral effect (which gives a negative contribution to the coefficient or rolling moment $C_{\mathcal{L}_\beta}$). As shown in the figure below, a side wind (i.e. sideslip) causes an overpressure under the upwind wing and therefore the aircraft tends to stabilize thanks to the rolling moment generated. On the other hand, low wings provide better aerodynamic performances due to the absence of the joints between wing and fuselage, needed for an high placement, and it means less interference drag. Moreover, it might help to reduce the take-off run taking advantage of the ground effect.

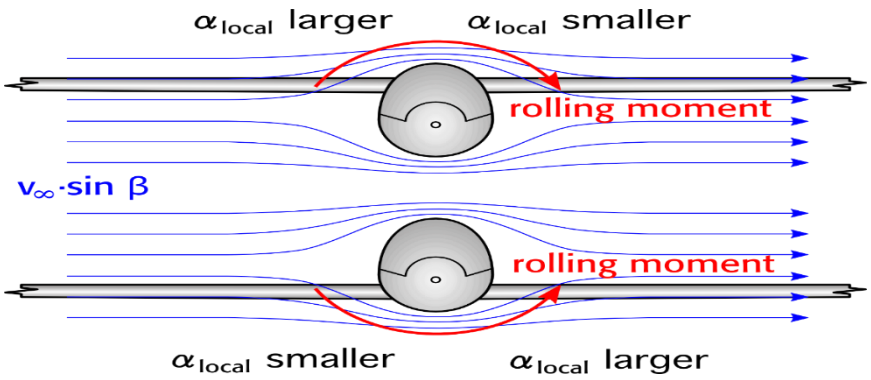

Figure 2-3. Dihedral effect

As regards reliability, in case of imprecise landing, the high wing configuration is safer because the clearance is greater than it is with the low wing one which, instead, may impact the ground in case of a high banking angle.

The most important feature of the low wing configuration is that it guarantees straightforward construction and simple access to the compartment where the passengers and luggage are stored. In addition, this configuration makes the assembly or substitution of the wing easier. On the contrary, with a high wing, the loading and unloading of the payload are likely to be more complex.

WING CONFIGURATION TRADE STUDY					
		HIGH		LOW	
Attribute	Weighting	Insert Score	Weighted score	Insert Score	Weighted score
Structural Weight	16%	0.4	0.064	1	0.16
Maneuverability	12%	0.6	0.072	0.8	0.096
Passengers Capability	20%	0.5	0.1	1	0.2
Speed	14%	0.4	0.056	0.7	0.098
Manufacturability	18%	0.6	0.108	0.9	0.162
Take-OFF Run	10%	0.5	0.05	0.8	0.08
Reliability	10%	0.9	0.09	0.4	0.04
Total	100%		0.54		0.836

Table 2-5. Wing positioning trade study

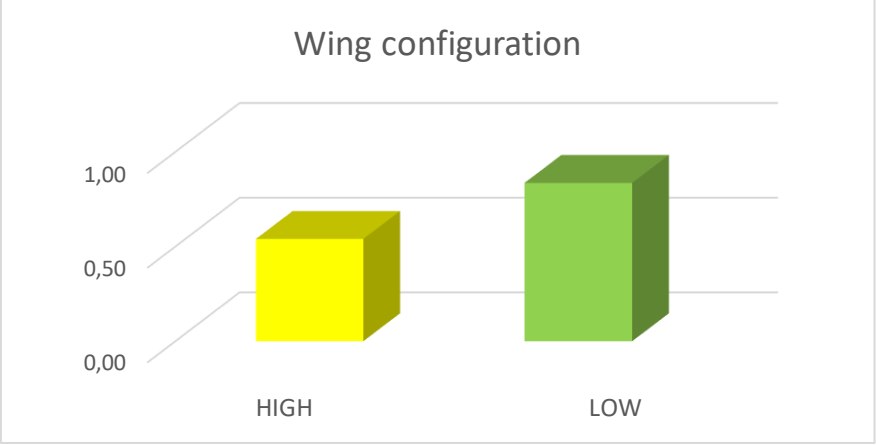

Figure 2-4. Wing configuration trade study

2.1.3 Tail

Once the configuration of the main wing is established, it is fundamental to discuss characteristics of the tailplane, specifically on a matter of stability, controllability, and reliability.

The main types of tailplanes currently adopted by the aerospace industry are conventional, T tails, and V tails. All of those options provide the aircraft with specific advantages and drawbacks that require careful analysis.

It seems clear that the weight of the structure that supports the aerodynamic surfaces of the tailplane won't be a major point of this discussion since it contributes only by a little percentage (estimated 5%) of the total inertial forces of the model aircraft.

The key point to analyze is, instead of how a different configuration plays into the overall stability and control of the aircraft, the effect that each one has on the take-off distance.

The T-tail is composed of a vertical stabilizer that holds, within itself, the support structure of the horizontal stabilizer, placed at its tip. This particular kind of tailplane offers the advantage of working in an undisturbed airflow, allowing it to generate more lift at a lower speed. Indeed, the dynamic pressure hitting the horizontal plane is unaffected by the downwash of the main wing. At the same time, the horizontal tail reduces the magnitude of the vertical tail tip vortex, increasing the vertical tail effectiveness in a sideslip, a phenomenon called the end-plate effect.

Many times these advantages are outshined by a safety flaw of the T configuration: in extreme stall conditions, the cone of turbulent flow coming from the main wing might engulf the tailplane, reducing its power of control turning it not effective altogether. This reason, along with an increased load on the Vertical stabilizer, brought the team to reject the T-tail configuration.
T-tail is also prone to flutter, a dynamic aeroelastic phenomenon that must be avoided to fly safely. Tail fluttering can rapidly destroy the empennage, leaving the aircraft without stability and control. To avoid fluttering, the T-tail must have a very strong and rigid structure, which will increase the structural weight, outshining its aerodynamic advantage.

In contrast with all standard configurations, the V-tail consists of only two aerodynamic surfaces, they are tilted on an angle and often fixed on the upper side of the aircraft, effectively getting rid of one of the three wings that form the usual tailplane design. This of course makes the tail lighter, but, as we previously discussed, that is not an important issue for the analysis. Once again, the focus is on the ability of this configuration to provide stability and control authority during flight. The main feature of the V-tail is that the control power of the rudder and equalizer is mixed and enforced using only two control surfaces. Yaw and Pitch are

consequently less effective unless the dimensions of the tail increase. This potential lack of power of the mixed equalizer might also result in a less effective take-off, which is one of the given requirements for the aircraft.

Therefore, the attention was focused on the conventional design for the tailplane. Both the deeper understanding of its properties and the possibility of installing a stabilator (provided only by this configuration) give this design an edge over the other two.

TAIL CONFIGURATION TRADE STUDY							
		T		Conventional		V	
Attribute	Weighting	Insert Score	Weighted score	Insert Score	Weighted score	Insert Score	Weighted score
Structural Weight	16%	0.7	0.112	1	0.16	0.5	0.08
Maneuverability	12%	1	0.120	1	0.120	0.2	0.024
Passengers Capability	20%	0	0.000	0	0.000	0	0.000
Speed	14%	0.8	0.112	1	0.140	1	0.140
Manufacturability	18%	0.75	0.135	1	0.180	0.1	0.018
Take-OFF Run	10%	1	0.100	1	0.100	0.25	0.025
Reliability	10%	0.7	0.070	1	0.100	0.2	0.020
Totals	100%		0.65		0.80		0.31

Table 2-6. Tail configuration trade study

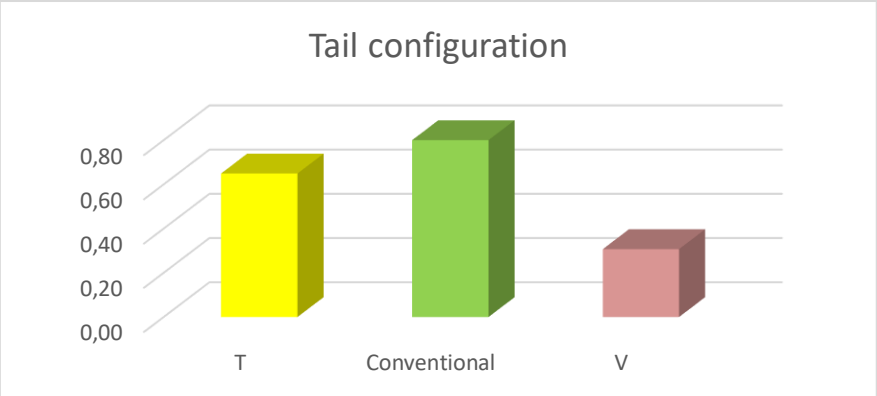

Figure 2-5. Tail configuration trade study

2.1.4 Number of Engines

Several factors were taken into account while conducting the propulsion system trade study for the aircraft. In particular, this section aims to understand what the best number of engines is to install on the aircraft and, therefore, choose either the single-engine configuration or the twin-engine configuration.

Firstly, it's been asserted that a single-engine configuration shall guarantee a certain overall weight saving since the battery pack should be lighter than the one needed for two engines. On the other hand, while a single-engine would be installed on the aircraft's nose, in the case of the twin-engine configuration, the engines would be installed on the wing structure. The presence of two inertial masses on the wing would make the total wing load decrease, thus the wing itself would be less stressed during flight. However, if the engines are installed on the wing, then a strengthened structure is needed where the engines are attached to the wing. That might mitigate the weight advantages aforementioned and would undermine the ease of manufacturing of the wing. Moreover, the CG of the wing sections that are behind the engine might shift ahead of the aerodynamic center. This increases the torque insisting on the wing structure.

The position of the engines also influences the maneuverability and stability of the aircraft. If the engine is on the aircraft's nose then it won't be influenced by the upwash generated by the wing therefore the phenomena of non-axial flow, derived by the interaction air-wing, can be ignored. Furthermore, the energized flow behind the propeller increases the efficiency of the aerodynamic surfaces both of the horizontal tailplane and, to a lesser extent, the main wing. However, a twin-engine configuration ensures better directional control as it is possible to realize a differential thrust to help the rudder in case of need. At the same time, two engines

require a bigger and strengthened rudder because it must guarantee directional controllability in the case of one inoperative engine.

From a safety standpoint, two engines installed on the wing might be an obstacle while loading and unloading passengers as they would be close to the fuselage part that needs to be open during ground operations. Thus, for this reason, and to guarantee a certain clearance from the ground, the propellers' diameter has to be limited. While it is true that in the case of one-engine-inoperative condition (OEI) a twin-engine configuration doesn't force the aircraft to abort the mission, it also requires a more complicated electrical system and one more channel on the aircraft's controller than the single-engine configuration. Two engines also imply more maintenance and greater difficulty in case of substitution or repair of one of the engines or the main wing.

It's not possible to decide without more specific considerations which configuration to choose. Therefore, once the aircraft geometry and structural characteristics will be more or less fixed, both studies about the single-engine and the twin-engine configuration will be further conducted to have a better understanding of the problem.

As shown by the following table, it's hard to pick the best configuration overall, so, this document will arbitrarily focus on the twin-engine configuration, considering both the effect that the two engines will have on the final weight of the aircraft and the impact on the main maneuvers.

ENGINE CONFIGURATION TRADE STUDY					
	N	single		twin	
Attribute	Weighting	Insert Score	Weighted score	Insert Score	Weighted score
Structural Weight	16%	1	0.16	0.5	0.08
Maneuverability	12%	1	0.120	0.3	0.036
Passengers Capability	20%	0.6	0.120	1	0.200
Speed	14%	0.5	0.070	1	0.140
Manufacturability	18%	1	0.180	0.75	0.135
Take-OFF Run	10%	0.7	0.070	1	0.100

Reliability	10%	0.5	0.050	1	0.100
Total	100%		0.77		0.79

Table 2-7. Engine configuration trade study

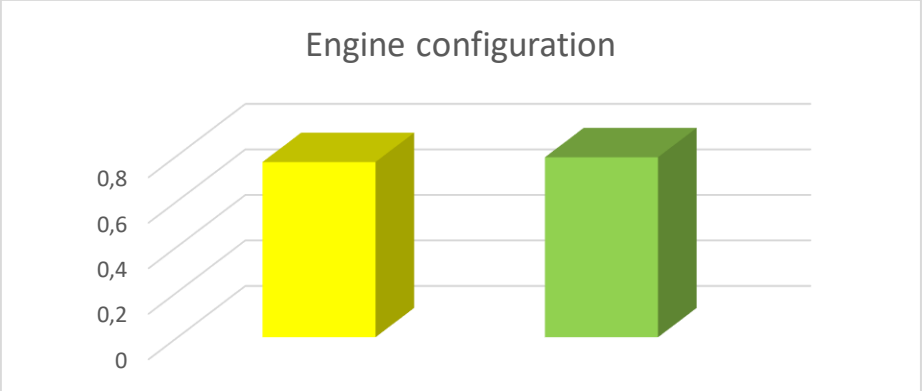

Figure 2-6. Engine configuration trade study

2.1.5 Landing Gear Type

Two different types of landing gear were compared. The first one is the tricycle landing gear that has a single nose wheel in the front, and two main wheels positioned close to the center of gravity. The other alternative is the bicycle landing gear, also known as "taildragger", which consists of a pair of wheels ahead of the center of gravity with an additional smaller wheel in the back of the plane.

By comparing the two solutions it was deduced that the tricycle leads to greater structural weight than the bicycle. However, the weight gap is not wide enough to consider this aspect as a key factor for choosing one over the other.

From the maneuverability point of view, it was found that the tailwheel-type landing gear, forces the aircraft to have a lower pitch angle during landing. That implies a strong use of the elevators to ensure a correct maneuver. Moreover, the relative position of CG and main landing gear doesn't mitigate the effect of the momentum generated by the friction between wheels and the runway. Therefore, the rudder needs to make the aircraft stable for the whole duration of the landing, even after the aircraft meets the ground. On the other hand, the tricycle landing gear allows the aircraft to fly at a greater AoA during the approach to the runway, reducing landing speed and making the landing maneuver safer. The tricycle is also more stable during

landing especially in the case of single-engine configuration, as it guarantees more support to the nose's structure that carries the propeller and the engine.

The two-wheeled gear is aerodynamically convenient because the area exposed to the airflow is less than it is in the tricycle configuration.

The final boardable number of passengers will not be significantly affected by one of the different configurations considered. However, the tricycle is more comfortable because it does not involve any inclination of the fuselage during ground operations, so it is easier to load/unload passengers.

In the case of the bicycle landing gear, there is a greater inclination between the aircraft and the ground which implies a drag increment and it complicates the take-off maneuver. This condition stands until the aircraft is aligned with the runway. The bicycle landing gear is also preferable on a grass airfield. On the other hand, the tricycle landing gear gives some advantages in terms of thrust during the take-off run because the thrust vector itself is parallel to the ground. That allows a greater acceleration to quickly reach lift-off speed. This alternative is most suitable for asphalted runways.

GEAR CONFIGURATION TRADE STUDY					
		BI		TRI	
Attribute	Weighting	Insert Score	Weighted score	Insert Score	Weighted score
Structural Weight	16%	1	0.16	0.8	0.128
Maneuverability	12%	0	0.000	0	0.000
Passengers Capability	20%	0	0.000	0	0.000
Speed	14%	1	0.140	0.95	0.133
Manufacturability	18%	0	0.000	0	0.000
Take-OFF Run	10%	0.7	0.070	1	0.100
Reliability	10%	0.5	0.050	1	0.100

Total	100%		0.42		0.46

Table 2-8. Landing gear configuration trade study

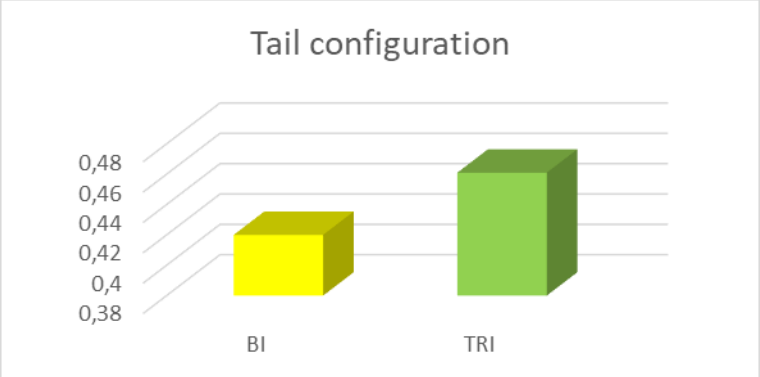

Figure 2-7. Tail configuration trade study

2.1.6 Fuselage

The key factor for the analysis of the fuselage is the amount of payload it can carry. The types of fuselages taken into account are:

- CLASSIC: lobe structure which allows defining a practical shell structure involving curved plated beams and fuselage former.

- SMOOTHED RECTANGULAR: rectangular structure characterized by several corners that allow the structure itself to absorb greater loads. This phenomenon, however, means that in those points there is a greater probability of cracks propagation.

The smoothed rectangular section has greater ease of construction and a better exploitability (more usable volume for a given section area) than the circular section.

FUSELAGE SECTION CONFIGURATION TRADE STUDY					
		SMOOTHED RECTANGULAR		CIRCULAR	
Attribute	Weighting	Insert Score	Weighted score	Insert Score	Weighted score
Structural Weight	16%	1	0.16	1	0.16
Maneuverability	12%	0	0.000	0	0.000
Passengers Capability	20%	1	0.200	0.75	0.150

Speed	14%	0.75	0.105	1	0.140
Manufacturability	18%	1	0.180	0.4	0.072
Take-OFF Run	10%	0	0.000	0	0.000
Reliability	10%	1	0.100	0.75	0.075
Total	100%		0.745		0.597

Table 2-9. Fuselage section configuration trade study

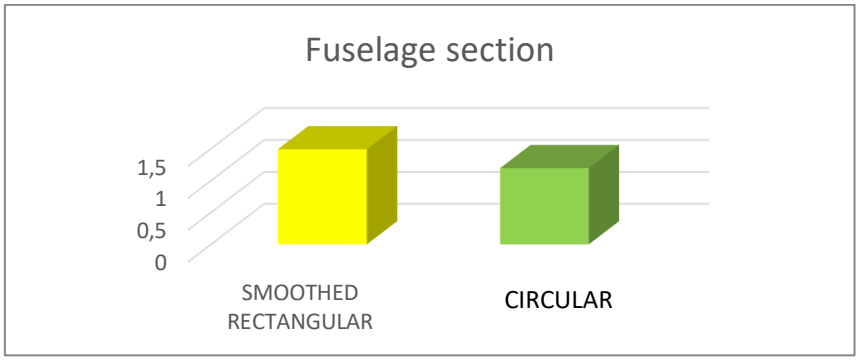

Figure 2-8. Fuselage section trade study

2.2 Sizing Process

Estimating the dimensions and weights of the aircraft is a crucial phase of the design process and it allows the team to develop more detailed analysis based on aerodynamics, structures, and flight performance. The sizing process consists of an iterative procedure that starts giving as input the wing load (statistically set), a plausible take-off and landing lift coefficient, and the distance of the take-off run according to the requirements. The process ends when the variation of the final weight assumes a value within the 3% compared to the previous iteration.

Before calculating the weights, the determination of the power loading $\frac{W}{\Pi}$, where W is the max take-off weight and Π is the engine max power, is essential. First of all, the stall speeds during landing and take-off are easily calculable knowing the density of the air, the wing load, and the two lift coefficients $C_{L_{max_L}}$ and $C_{L_{max_{TO}}}$.

After that, according to the constraint about the take-off distance, it is possible to establish the thrust-to-weight ratio by using the simplified formula of the take-off run as it follows:

$$S_G = \frac{1.21\ W/S}{\rho g C_{L_{max_{TO}}} T/W} \quad \rightarrow \quad \frac{T}{W} = \frac{1.21\ W/S}{\rho g C_{L_{max_{TO}}} S_G}$$

Since the electric engine is a propeller, it has been taken into account the power instead of the thrust during calculations. A proper approximation in take-off conditions is:

$$T = \frac{\Pi \eta_p}{0.7 \cdot 1.21 V_{S_{TO}}}$$

Furthermore, assuming a propeller efficiency η_p value relatively low (between 0.5 and 0.6), the following relation has been considered:

$$\frac{\Pi}{W} = \frac{0.7 \cdot 1.21^2\ W/S\ V_{S_{TO}}}{\eta_p \rho g C_{L_{max_{TO}}} S_G}$$

2.2.1 Weight Estimation

The characteristic weights of the aircraft are estimated in the following way.

The total weight (*W*) is given by the sum of different parts: structure, payload, engine (including propellers), batteries, electronic parts. Passengers and their luggage constitute the payload to carry. They are respectively represented by standard cylinders and parallelepipeds made of wood. Their single weight is established by the requirements.

$$W = W_{\text{struct}} + W_{\text{payload}} + W_{\text{engine}} + W_{\text{batteries}} + W_{\text{electronic pts.}}$$

The structure's weight can be expressed by the following relation which takes into account the weight of the different structural components:

$$W_{\text{struct}} = W_{\text{wing}} + W_{\text{fuselage}} + W_{\text{h-tail}} + W_{\text{v-tail}} + W_{\text{gear}}$$

It is possible to statistically determine these weights by considering other aircraft with similar manufacturing characteristics (i.e. aircraft made of balsa wood). Then it is possible to evaluate for each component the weight to area ratio W_{comp}/S_{ref} where S_{ref} is a characteristic surface of

the component itself. That surface will be represented by the planform area for the wing and by the product of diameter and length for the fuselage (or eventually only for the length of the part with a constant cross-section). The landing gear data can be obtained from statistics or relating it to the total weight. The $S_{h\text{-}tail}$ is considered as the 20-30% of the S_{wing}

$$\frac{W_{\text{wing}}}{S_{\text{wing}}} \quad \frac{W_{\text{fuselage}}}{D_{\text{fuselage}} L_{\text{fuselage}}} \quad \frac{W_{\text{h-tail}}}{S_{\text{h-tail}}} \quad \frac{W_{\text{v-tail}}}{S_{\text{v-tail}}} \quad \frac{W_{\text{gear}}}{S_{\text{gear}}} \quad \left(\text{or } \frac{W_{\text{gear}}}{W}\right)$$

The structure weight relation can be then developed by using these ratios as it follows:

$$W_{\text{struct}} = \frac{W_{\text{wing}}}{S_{\text{wing}}} S_{\text{wing}} + \frac{W_{\text{fuselage}}}{S_{\text{fuselage}}} S_{\text{fuselage}} + \frac{W_{\text{h-tail}}}{S_{\text{h-tail}}} S_{\text{h-tail}} + \frac{W_{\text{v-tail}}}{S_{\text{v-tail}}} S_{\text{v-tail}} + \frac{W_{\text{gear}}}{S_{\text{gear}}} S_{\text{gear}}$$

An iterative process is necessary as the surfaces considered before are initially unknown. Firstly, the values of the areas are hypothesized, then the weights of the single components are estimated as well as the total weight. Thus, the wing surface and the engine's weight can be determined by using the wing load and the power load previously obtained. The process explained is repeated until the difference between two consecutive iterations is less than 10g.

It is assumed a wingspan of 5 ft by referring to the constraints given by the requirements and a value for the aspect ratio (i.e. 8). It is also considered a rectangular wing because of its ease of manufacturing and its cost benefits:

$$AR = \frac{b^2}{S} \quad S = \frac{b^2}{AR} \quad S = bc \quad c = \frac{S}{b}$$

At this point, it is necessary to check whether the chord's length obtained is realistic comparing it to the fuselage one. While the length and diameter of the fuselage depend on the payload, the tail and nose lengths are statistically determined by considering the ones of similar aircraft.

As the structure weight is now known, the weight of electronic parts, engines, and batteries needs to be defined. This is possible by using catalogs on the internet which associates the maximum power supplied by the engine to its weight and recommended electronic parts, such as ESC and batteries. The following ratios can be then determined assuming an initial power of 300-600 W:

$$\frac{W_{engine}}{\Pi} \quad \frac{W_{\text{batteries}}}{\Pi} \quad \frac{W_{\text{electronic pts.}}}{\Pi}$$

Table 2-10. Iterations for weight estimation

ITERATIONS									
		ITERATION N. 1		**ITERATION N. 2**		**ITERATION N. 3**		**ITERATION N. 4**	
Name	**Symbol**	**Value**	**Unit**	**Value**	**Unit**	**Value**	**Unit**	**Value**	**Unit**
Power needed	Πn	153.71	W	156.43	W	157.22	W	157.44	W
ENGINE SYSTEM WEIGHT CALCULATION									
Engines weight	$W_{engines}$	0.091	Kg	0.092	Kg	0.093	Kg	0.093	Kg
Battery weight	$W_{battery}$	0.110	Kg	0.112	Kg	0.112	Kg	0.113	Kg
ESC weight	W_{ESC}	0.032	Kg	0.033	Kg	0.033	Kg	0.033	Kg
Engine Syst. weight	$W_{engine.pts}$	0,233	Kg	0.237	Kg	0.238	Kg	0.239	Kg
STRUCTURAL WEIGHT CALCULATION									
Wing surface	S_{wing}	0.298	m^2	0.303	m^2	0.305	m^2	0.305	m^2
Fuselage diameter	D_{fus}	0.130	m	0.130	m	0.130	m	0.130	m
Fuselage length	L_{fus}	0.738	m	0.738	m	0.738	m	0.738	m
Horizontal tail surface	S_{H_tail}	0.060	m^2	0.061	m^2	0.061	m^2	0.061	m^2
Vertical tail surface	S_{V_tail}	0.021	m^2	0.021	m^2	0.021	m^2	0.021	m^2
Structural weight estimate	W_{struct}	1.429	Kg	1.440	Kg	1.443	Kg	1.444	Kg
Payload weight	$W_{payload}$	1.371	Kg	1.371	Kg	1.371	Kg	1.371	Kg
Total aircraft weight	W_{tot}	3.033	Kg	3.048	Kg	3.053	Kg	3.054	Kg
CHECK									
Chord	c	0.199	m	0.202	m	0.203	m	0.204	m
Weight variation	ΔW	0.053	Kg	0.015	Kg	0.004	Kg	0.001	Kg

Table 2-11. Payload data input

PAYLOAD INPUT			
Name	**Symbol**	**Quantity**	**Unit**
Number of passengers	n	8	
Number of passengers for each row	N	2	
Passenger's length	a	0.031	m
Passenger's width	c	0.031	m
Passenger's height	l	0.09	m
Passenger's weight	M	113.4	g
Luggage length	a	0.019	m
Luggage width	c	0.025	m
Luggage height	l	0.038	m
Luggage weight	M	58	g

LEGEND	
Input Data	
Iterations results	

Table 2-12. preliminary aircraft data input

AIRCRAFT DATA INPUT			
Name	**Symbol**	**Quantity**	**Unit**
Wing Load	W/S	10	Kg/m^2
		98	N/m^2
Maximum landing lift coefficient	$CL_{max\_landing}$	1.8	
Maximum take-off lift coefficient	$CL_{max\_takeoff}$	1.5	
Take-off run	s_g	7.0	m
Wingspan	b	1.5	m
Aspect Ratio	AR	8.0	

Table 2-13. Conceptual design choices and payload parameters for first iteration

DESIGN			
Name	**Symbol**	**Quantity**	**Unit**
Stall speed - Landing	$V_{stall\_landing}$	3.0	m/s
Rate Thrust - Weight	T/W	0.0959	N/kg
Stall speed – Takeoff	V_{stall_TO}	3.3	m/s
Rate Power-Weight	Π/W	5.257	W/N
	Π/W	51.57	W/Kg
Structural Weight + Payload Weight	$W_{struct+payload}$	2.764	Kg
Structural Weight	W_{struct}	1.393	Kg
Payload Weight	$W_{payload}$	1.371	Kg
Power Required	Π_n	142.6	W
Electronics Weight	W_{elect}	0.159	Kg
Total Starting Weight	W_{tot}	2.923	Kg

PAYLOAD STRUCTURE INFORMATION			
Name	**Symbol**	**Quantity**	**Unit**
Number of rows	N	4	
Passenger and Luggage seat length	a1	0.060	m
Passenger and luggage seat width	c1	0.037	m
Passenger and luggage height	H	0.108	m
Total length of payload grid	A	0.240	m
Total width of payload grid	C	0.074	m
Final length of payload grid	A_{final}	0.264	m
Final width of payload grid	C_{final}	0.081	m
Front part length	r	0.204	m
Tail length	j	0.270	m
Aircraft Length	L	0.738	m
Payload Weight	$W_{payload}$	1371.2	g

STATISTIC ESTIMATION			
STRUCTURAL WEIGHT ESTIMATION			
RATIOS ESTIMATION			
Name	**Symbol**	**Quantity**	**Unit**
Wing's ratio	W_{wing}/S_{wing}	1.8300	[Kg/m^2]
Fuselage's ratio	$W_{fus}/(D_{fus}*L_{fus})$	8.3000	[Kg/m^2]
Horizontal taiplane's ratio	W_{H_tail}/S_{H_tail}	1.0600	[Kg/m^2]
Vertical tailplane's ratio	W_{V_tail}/S_{V_tail}	1.2500	[Kg/m^2]
WEIGHTS ESTIMATION			
Name	**Symbol**	**Quantity**	**Unit**
Wing surface	S_{wing}	0.2813	m^2
Fuselage diameter	D_{fus}	0.1296	m
Fuselage lenght	L_{fus}	0.7383	m
Horizontal tailplane surface	S_{H_tail}	0.0563	m^2
Vertical tailplane surface	S_{V_tail}	0.0197	m^2
Structural Weight	W_{strutt}	1.393	Kg

Table 2-14. Empirical data for weight estimation

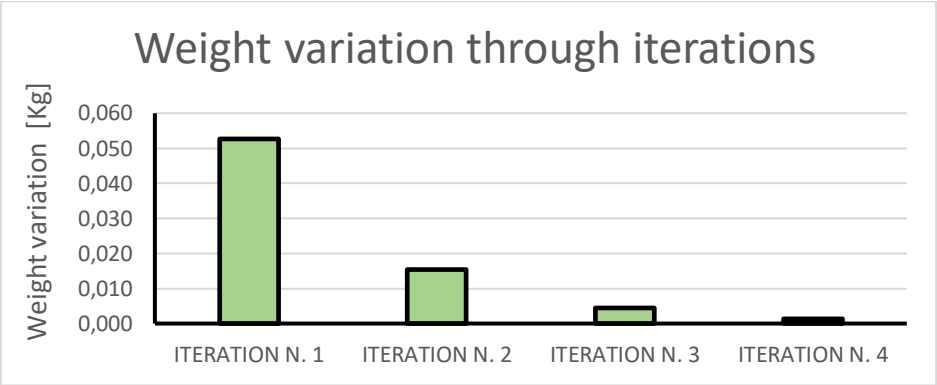

Figure 2-9. Convergence of iterations

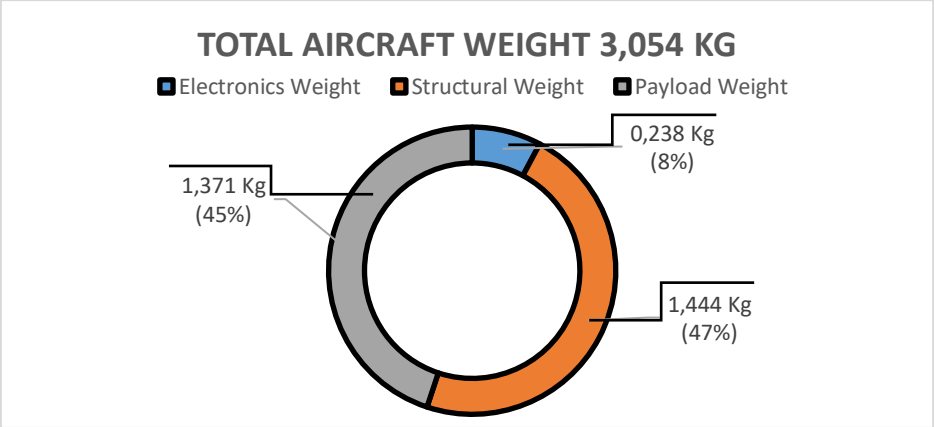

Figure 2-10. Post-iterations Aircraft Weight

This final value of the weight provides the Team a weight requirement for the electronics, allowing the selection of a proper setup. As stated in *paragraph 2.1.4*, this paper focuses on a Twin-Engine configuration, so the electronics system and the propulsion system have to fit that layout.

The components chosen, that will provide the basis in terms of power for the discussions in *Chapter 3*, are:

- Two "A20-30M EVO kv980" brushless engines from *Hacker*
- One lipo battery "25C ECO-X 1300mAh 3S MTAG" from *TopFuel*
- Two Speed controller X-12-Pro with BEC (ESC)

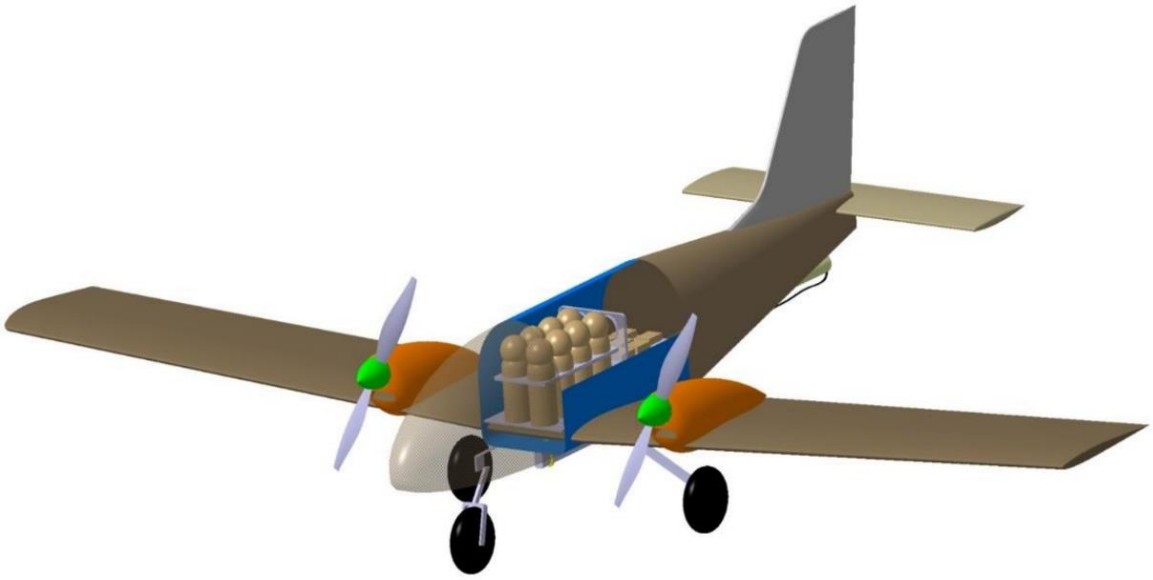

3 Chapter 3 - Main flight performances and maneuvers

Once the main configuration of the aircraft has been established, the next logical step was to evaluate how those choices affected the overall performances, with special care given to the parameters that most influence the score of the competition.

With that purpose, this chapter will focus on the main maneuvers that the aircraft will be performing during the nominal flight course proposed by the competition and will provide a detailed analysis of the estimated behavior of the aircraft for each of them.

The main parameters that will remain constant throughout *Chapter 3* are the following:

Unloaded combined shaft power	Π_0	157 W	(80% of maximum power)

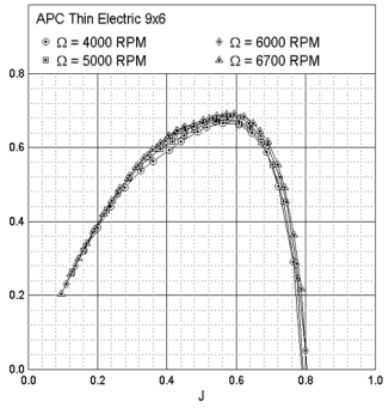

Figure 3-1. Propeller efficiency vs J

The selected propeller is the *APC thin electric 9x6*, small enough to provide the ground clearance needed.
On the left is the graph showing the dependence of the propeller efficiency (η_p) with J.

$$J = \frac{V}{nD}$$

n: Revolutions per second; D: Propeller diameter; V: asymptotic speed

3.1 Take-off Run

While dealing with the Take-off run, the main thing we must consider is the limitation given to us by the requirement section (see *Chapter 1.0.1*), forcing us to clear the ground within seven meters from the starting line.

Take-Off Run	$23\ ft = 7\ m$

To make sure that this parameter is satisfied, it is important to calculate when the aircraft will reach its lift-off speed (V_{LO}) and, given that information, the space required to reach that speed.

The reader will find within this chapter the calculations regarding both the ground roll, which is subjected to the requirements, and the take-off air distance (or transition).

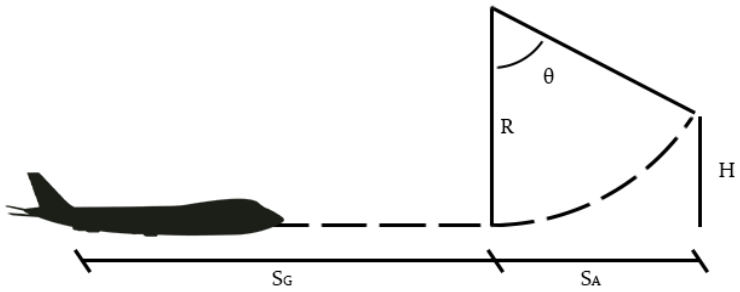

Figure 3-2. Take-off run diagram

3.1.1 Ground Roll S_G

While studying the dynamics of the take-off, we must consider that the standard polar of the aircraft cannot be utilized, that is both because there are more than aerodynamics forces involved and because the CD0 of the aircraft changes while in the take-off configuration (added drag from flaps and landing gears).

$$C_{Dg} = C_{D0} + \Delta C_{D0_{flap}} + \Delta C_{D0_{L.gear}} + \frac{{C_{Lg}}^2}{\pi \cdot AR \cdot e} * K_{ES}$$

With this information, we can apply a forces balance equation involving lift, drag, thrust, and friction resistance from the wheels to solve for the acceleration, crucial in the following observation:

$$S_G = \int_0^{V_{LO}} dS = \int_0^{V_{LO}} \frac{VdV}{a} \cong \frac{1}{2}\int_0^{V_{LO}} \frac{dV^2}{\bar{a}}$$

The parameter $\bar{a}$ is the mean value of the acceleration of the aircraft, whose components are calculated at 70% of V_{LO}.

By virtue of previous aerodynamics studies through OPEN VSP, the Lift Coefficient of the aircraft when in ground configuration is known (C_{LTO} = 1.5), that value, paired with the final weight of the aircraft and the data coming from the sizing process, allows calculating the stall speed.

$$V_{stall} = \sqrt{\frac{2}{\rho} \cdot \frac{W}{S} \cdot \frac{1}{C_{L_{maxTO}}}} = 3.27 \frac{m}{s}$$

Considering that the pilot needs a speed marginally superior to the V_{stall} to rotate the aircraft and lift off, it's conscious to assume the following:

$$V_{LO} = 1.1 \cdot V_{stall} = 3.60 \frac{m}{s}$$

We now have the foundation to evaluate the Ground Roll:

$$S_G = \frac{W}{2g}\int_0^{V_{LO}} \frac{dV^2}{[T - D - \mu(W - L)]} \cong \frac{W}{2g} \cdot \frac{{V_{LO}}^2}{[T - D - \mu(W - L)]|_{0.7\,V_{Lo}}} = 4.92\ m$$

The main assumption is considering the main forces acting on the aircraft during the take-off as constants, particularly using their value at 70% of the lift-off speed.

The reader can consult the following table and chart for a clear representation of the forces acting on the aircraft.

Available Power	108.3	[W]
Mean Friction drag (at 70% of VLO)	0.70	[N]
Mean Aerodynamic Drag (at 70% of VLO)	1.15	[N]
Mean Thrust (at 70% of VLO)	43.64	[N]

Table 3-1. Mean forces at take-off

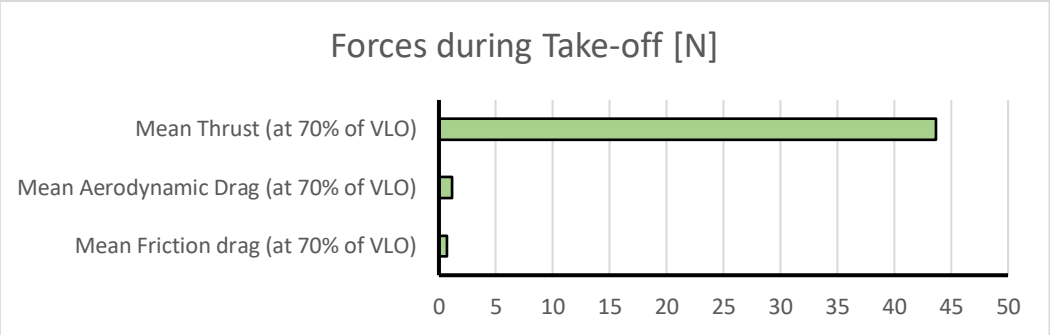

Figure 3-3. Comparison between mean forces at Take-off

The Team is satisfied with the estimated ground roll distance since it is beneath the limitation by an acceptable margin.

3.1.2 Transition Phase

Once the aircraft leaves the ground there is a temporary phase meant to safely clear the runway.

For this purpose, an imaginary obstacle with a fixed height (H) is put further down the runway, with the intent of being flown over.

It will be assumed that, during the Transition Phase, the aircraft will fly almost at stall condition, with the proper safety margin, thus knowing the lift coefficient, we can estimate the load factor (n), which will consequentially give a measure of how much lift the aircraft is generating, compared to its weight.

$$n = \frac{L}{W} = 1.189$$

With an equilibrium equation involving the radial forces during the maneuver we can calculate the flare radius (as shown in Figure 3-2):

$$R = \frac{V^2}{g \cdot (n-1)} = 7.59\, m$$

Simply by geometrical means, we can now evaluate the angular distance that the aircraft will cross on that circumference, and, with that, also the horizontal distance that it will have traveled.

With an obstacle height of 0.4 meters:

$$\theta = \cos^{-1}(1 - \frac{H}{R}) = 0.326\, rad$$

Estimated take-off air distance:

$$S_A = R \cdot \sin\theta = 2.43\ m$$

Total Take-off run:

$$S_{TOT} = S_A + S_G = 7.35\ m$$

3.2 Climb

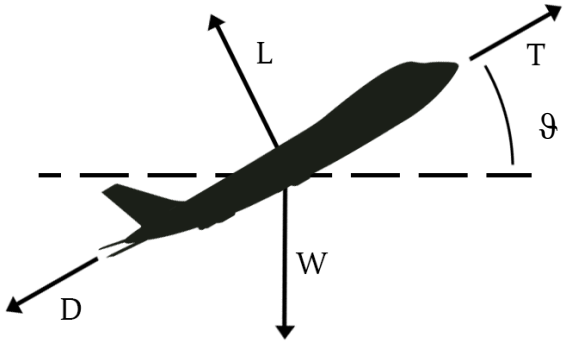

Figure 3-4. Climb diagram

By the nature of the competition, both speed and safety are key factors. Because of that principle, the Team decided to select a flight path that would clear the ground as fast as possible, but to minimize the risk of incidents with ground objects, the angle of climb (ϑ) must be high too.

For that reason, it is important to evaluate the hodograph, a diagram that compares the Rate of Climb (RC) with the horizontal velocity (V_H) of the aircraft, and, within it, finding both the speed that maximizes the vertical speed and the one that allows the steepest angle of climb.

$$RC = \frac{dh}{dt} = V_\infty \cdot \sin\vartheta$$

(ϑ) Angle of climb, formed between the flight path and the horizontal direction.

By applying an equilibrium equation of the longitudinal forces acting on the aircraft, it is possible to solve the resulting equation for the RC, concluding that the Rate of Climb is proportional to the exceeding power provided by the engines.

$$T = D + W\sin\vartheta \rightarrow RC = \frac{T \cdot V_\infty - D \cdot V_\infty}{W}$$

Evaluating the RC for each velocity above the V_{stall} allows finding two very important climbing conditions, both visible in the hodograph.

INPUT Parameters:		
C_{DO}	0.003	
ARe	6.4	
Atmospheric density	1.225	[kg/m^3]
Weight	3.05	[Kg]
Vstall	3.3	[m/s]
φ (power level)	1	
Propeller efficiency	69%	
Unloaded shaft power	157	[W]

Table 3-2. Boundary conditions for Rate of Climb estimation

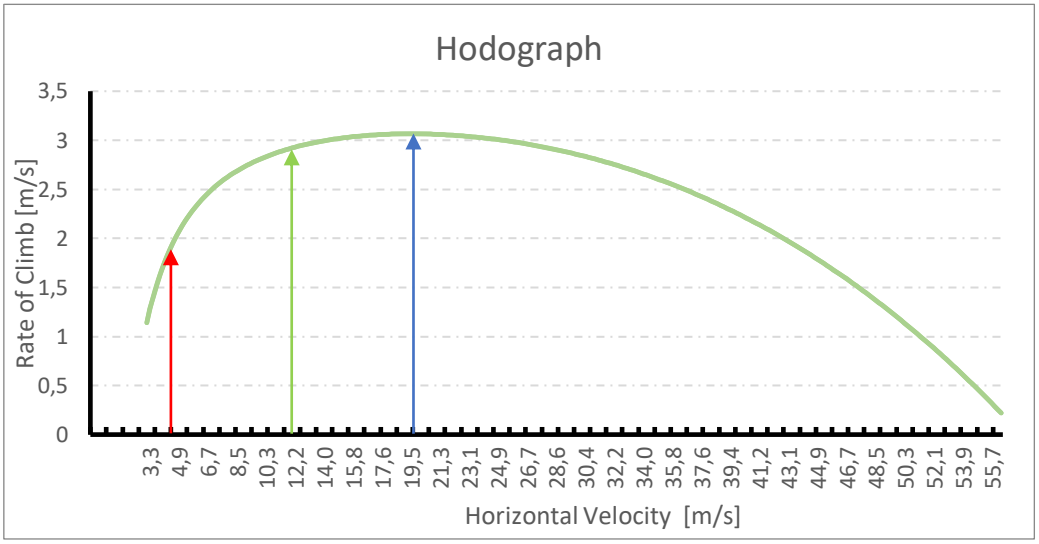

Figure 3-5. Hodograph of climb

By analyzing all the possible climbing conditions, the main two settings for the pilot to consider are the “Steepest climb”, pointed in red in the Hodograph, and the “Fastest climb”, noted in blue.

The parameters for both of those conditions are in the following table, along with the final configuration chosen for the competition, highlighted in green, that will preserve a good amount of horizontal velocity while keeping a high angle of climb, to avoid any possible ground obstacles.

Asymptotic Velocity V_∞ [m/s]	Rate of Climb [m/s]	Angle of Climb ϑ [deg]
19.7	3.07	8.95
4.5	1.8	23.57
Adopted Configuration:		
12	2.9	13.9

Table 3-3. Fast and steep climb parameters

The horizontal axis of the Hodograph is purely ideal, the model aircraft will have a theoretical maximum speed far lower than what is shown, as explained in the *Paragraph 3.3*.

3.3 Maximum Velocity

Since the flight path dictated by the competition has within it a 1000 ft long straight, it is reasonable to assume that most of that section will be traveled at the aircraft's maximum velocity.

To estimate that value it is imperative to recognize what are the key characteristics of the aircraft that will most affect it, those being the power that the engine provides to the aircraft, the efficiency of the propeller, and the drag parameters.

Assuming that the pilot will keep the throttle at the maximum value, it is possible to calculate the available power:

$$\Pi a = \Pi_0 \cdot \varphi \cdot \eta_p = 102.1\ W$$

(Πa) Available power.
(Π_0) Power provided to the unloaded shaft.
(φ) Throttle.
(η_p) efficiency of the propeller, from the aerodynamics team's data, assumed to be 0.65.

By virtue of this result, to obtain the maximum speed that the aircraft can nominally sustain in level flight, it must be evaluated the power needed for each velocity condition. The resulting speed at which power dependence (Πn) matches the maximum power available (Πa) represents the maximum velocity (V_{max}) of the aircraft.

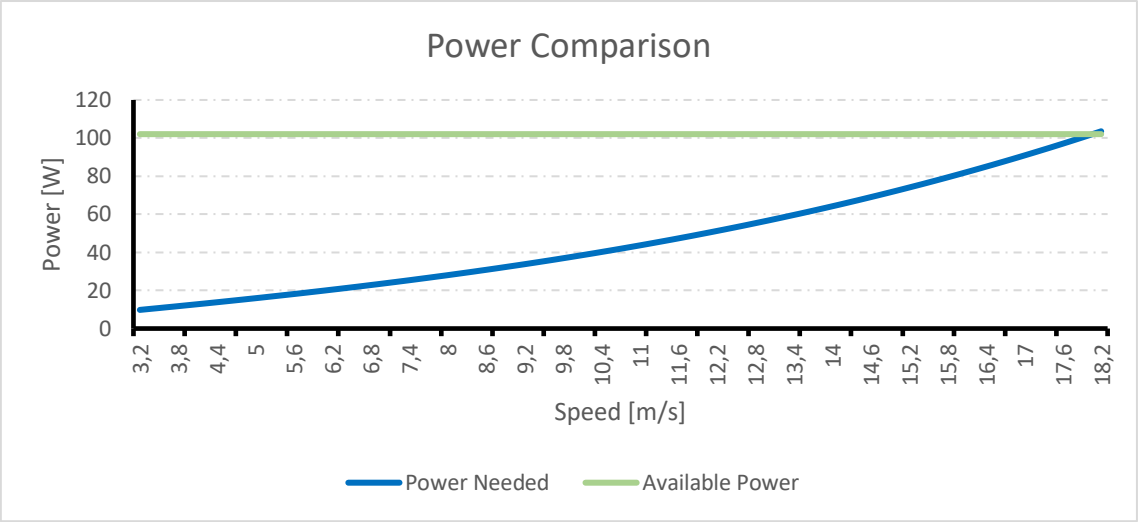

Figure 3-6. Power needed vs available power

Being the powertrain electric, it is safe to assume that the available power is not dependent on the altitude, therefore a constant.

From those data it is possible to obtain the theoretical maximum speed:

Power Needed Πn [W]	Throttle φ	Vmax [m/s]
101.3	100%	18

It might help the pilot know how the aircraft performs at different levels of throttle configuration, because of that, the reader will find the diagram showcasing the different maximum speeds paired to its level of throttle.

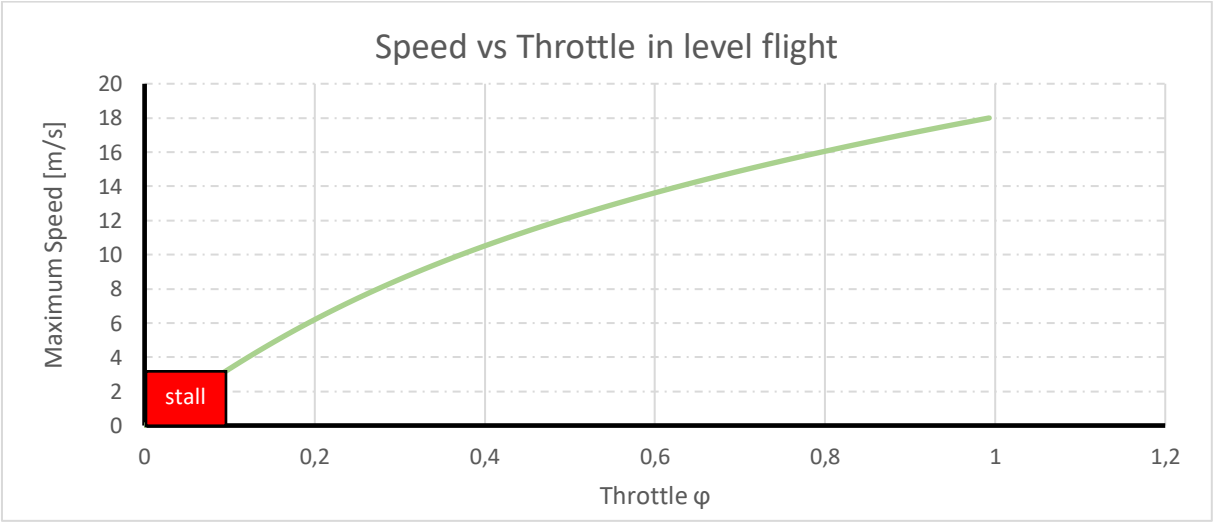

Figure 3-7. Speed vs throttle graph

3.4 Glide

As required from the competition rulebook, the last approach to the landing site must be attempted while keeping the engines idle, which will consequentially cause the aircraft to switch from powered flight, in favor of a temporary gliding phase.

To predict how the trajectory on the final approach might look like, here the reader will find an analysis of unpowered flight, with particular care given to the Sink Rate (SR), the vertical speed of the aircraft.

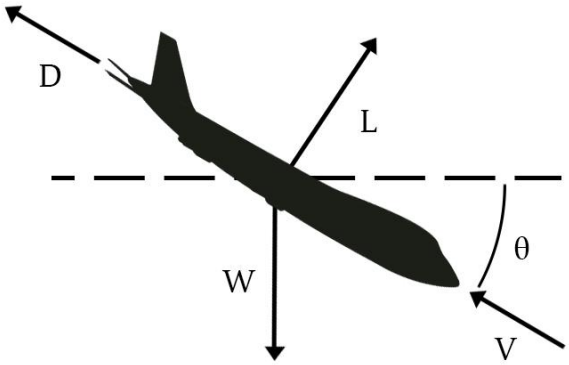

Figure 3-8. Glide diagram

From geometric consideration, we can find an equation for the Sink angle (ϑ).

$$\begin{matrix} L = W\cos\theta \\ D = W\sin\theta \end{matrix} \rightarrow \tan\theta = \frac{1}{L/D} = \frac{1}{E}$$

With this consideration, to glide with the lowest possible Sink Angle, the aircraft must fly at its most efficient attitude.

To understand what that would imply, it's important to find, within the polar diagram, the point, known as "E" of maximum efficiency.

With the following observation and the value of the Zero-lift Drag Coefficient given to us by the aerodynamics team, supported by various CAE programs (mainly OPEN VSP), we can generate the diagram for the polar of the aircraft.

$$C_D = C_{D0TOT} + \frac{{C_L}^2}{\pi \cdot AR \cdot e}$$

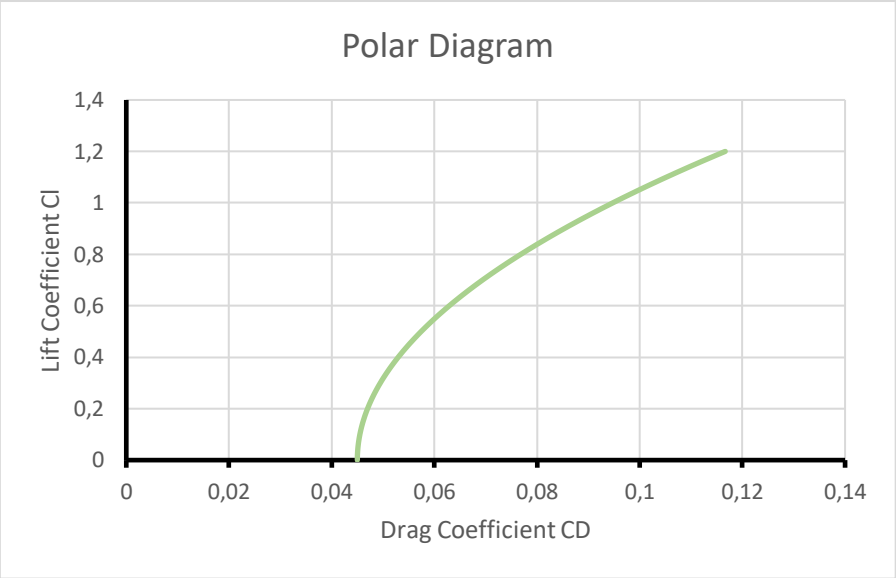

Figure 3-9. Estimated polar diagram

It is now possible to extrapolate the value of the efficiency at the various attitudes, which will allow the estimation of the minimum Sink Angle and the minimum Sink Rate through the following procedure:

$$in\ equilibrium\ conditions:$$
$$SR = V_\infty \cdot \sin\vartheta$$
$$D = W \cdot sin\vartheta$$
$$V_\infty = \sqrt{\frac{2\cos\vartheta}{\rho \cdot S \cdot C_L}} \cdot \sqrt{\frac{W}{S}} \quad \rightarrow SR = \frac{D \cdot V_\infty}{W} = \frac{\Pi_n}{W}$$

We now can identify the behavior at the maximum efficiency attitude, that will result in the lowest Sink Angle:

$$\vartheta_{min} = \tan^{-1}\left(\frac{1}{E_{max}}\right) = 5.41\ deg$$

Furthermore, with those data, we can evaluate, for each attitude, the one that minimizes the power needed to fly, therefore the Sink Rate:

$$\mathrm{SR}_{min} = \left.\frac{\Pi_n}{W}\right|_{min} = -1.13\ {}^{m}/_{s}$$

That can be achieved by flying with an AoA of 13° (Data acquired by using the C_L-AoA diagram of the aircraft).

The reader is presented with the general Sink Rate diagram:

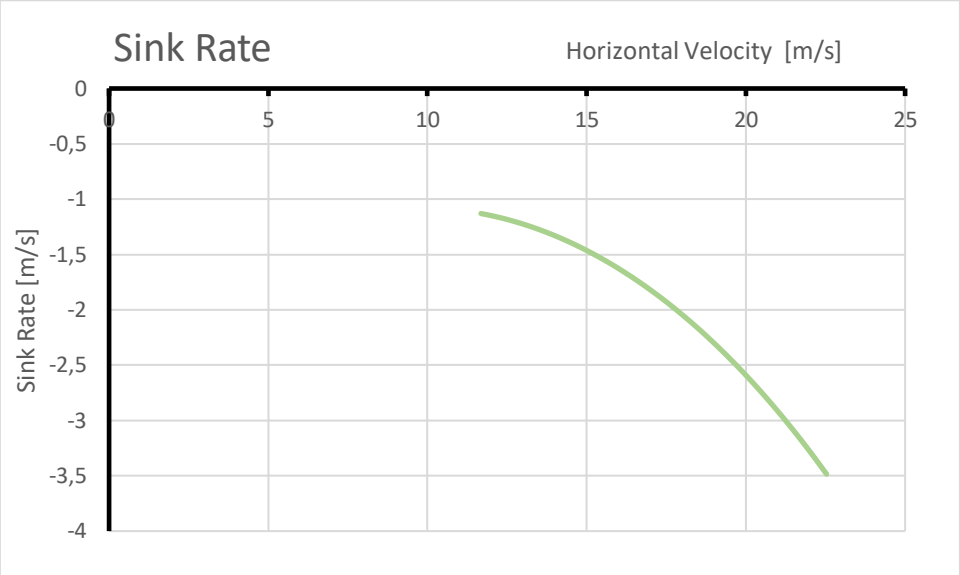

Figure 3-10. Sink rate diagram

3.5 Turn

The flight path established by the competition forces to reverse the horizontal direction twice and, for that reason, it is important to comprehend the behavior of the aircraft during banking maneuvers.

Key aspects of this analysis are the banking radius (R), the banking angle (ϕ), and the turning angular velocity (ω).

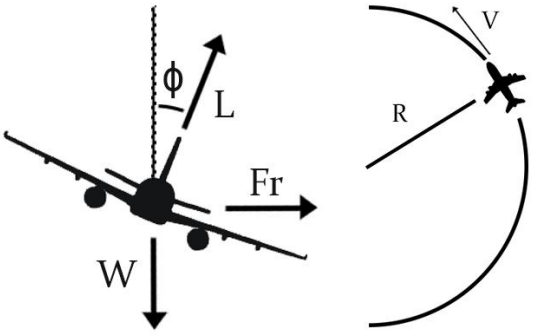

Figure 3-11. Turn diagram

To find out if the aircraft is capable of following the nominal path of the flight course during the turning, it's important to fix the parameters of said maneuver. Those are determined by ruleset, structural limits of the aircraft, and empirical data for banking maneuvers of other model airplanes of similar powertrain, and they are as follows:

V_{turn}	13 [m/s]
R	10 [m]
n_{max}	3.8

Table 3-4. Competition and structural Requirements for turning maneuver

Given those parameters we can evaluate how much the rulebook's proposed turn will stress the structure of aircraft by calculating the load factor, assuming a stabilized turn.

(n) Load factor. $n = \frac{L}{W}$

Since the centrifugal force must equal the centripetal force (see *Fr* in Figure 3-11) in a stabilized maneuver, we can arrive at the following conclusion:

$$\text{Fr} = \sqrt{L^2 - W^2}$$
$$Fr = \frac{W}{g} \cdot \frac{{V_{turn}}^2}{R} \quad \rightarrow \quad R = \frac{{V_{turn}}^2}{g \cdot \sqrt{n^2 - 1}} \quad \rightarrow \quad n = 1.99$$
$$n = \frac{L}{W}$$

Having established that the value of the load factor is far beneath the maximum bearable by the aircraft structure, it is possible to calculate the banking angle that the pilot will have to set.

$$\phi = \cos^{-1}\left(\frac{1}{n}\right) = 59.83\ deg$$

We can showcase the dependence of the load factor with the banking angle to obtain the maximum bearable attitude:

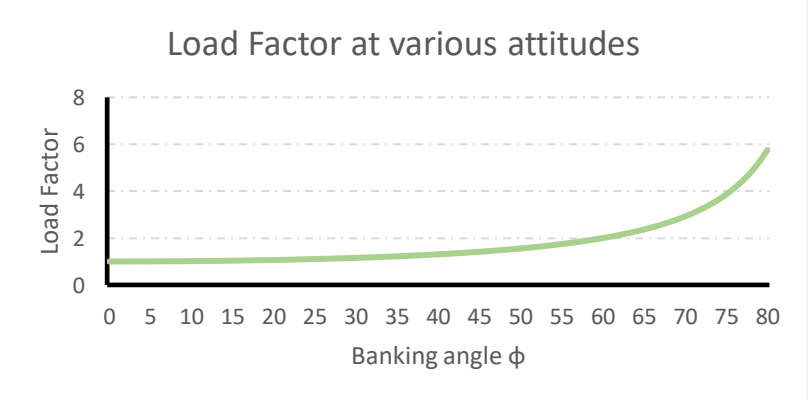

Figure 3-12. Load Factor vs attitude graph

$$n_{max} = 3.8 \quad \rightarrow \quad \phi_{max} = 74.75\ deg$$

In case of emergency, the pilot might need to follow a tight trajectory, it is, therefore, important to evaluate the minimum possible turning radius (R_{min}).

Having established the quadratic dependence of the turning radius with the turning velocity, it's clear that a tight turn will be performed at near-stall conditions.

While calculating the stall speed, it must be considered that there is a component of lift that is not opposing gravity, creating a dependence of the stall speed with the banking angle, therefore with the load factor as follows.

$$V_{stall\_turn} = \sqrt{\frac{2}{\rho} \cdot \frac{n_{max} \cdot W}{S} \cdot \frac{1}{C_{L_{max}}}} = 7.00\ {}^{m}/_{s} \rightarrow \begin{matrix} R_{min}|_{n_{max}} = 1.36\ m \\ \omega_{max} = \dfrac{g \cdot \sqrt{n^2 - 1}}{V_{stall\_turn}} = 5.13\ {}^{rad}/_{s} \end{matrix}$$

(ρ) Air density at sea level.

(S) Wing planform area.

($C_{L_{max}}$) Maximum Lift Coefficient with standard in-flight configuration. $C_{L_{max}} = 1.3$

(ω_{max}) Maximum turning angular velocity.

From the polar diagram, it can be obtained the efficiency of the aircraft during the turning maneuver, which will be useful to calculate the power needed to perform it.

It is important to remember that during a turn, aerodynamic drag increase proportionally with the load factor. With that in consideration we can calculate the power needed for the tightest turn:

$$\Pi_{n\_turn} = D_{turn} \cdot V_{turn} = \frac{n_{max} \cdot W}{E} \cdot \sqrt{\frac{2}{\rho} \cdot \frac{n_{max} * W}{S} \cdot \frac{1}{C_{L_{max}}}} = 79.1\ W$$

(E) Efficiency of the Aircraft at maximum attitude. $E = 10.07$

The found value is the highest that any stabilized turn could require, thus proving that the aircraft is capable of performing the turning maneuver necessary for the competition.

3.6 Landing

By the competition rulebook, the landing phase of the flight curse is not counted for the final timing of the laps. That allows for a slow and safe landing which phases are going to be discussed in the following pages, intending to inform the pilot about the correct attitude and flight configuration to minimize the stress upon the aircraft.

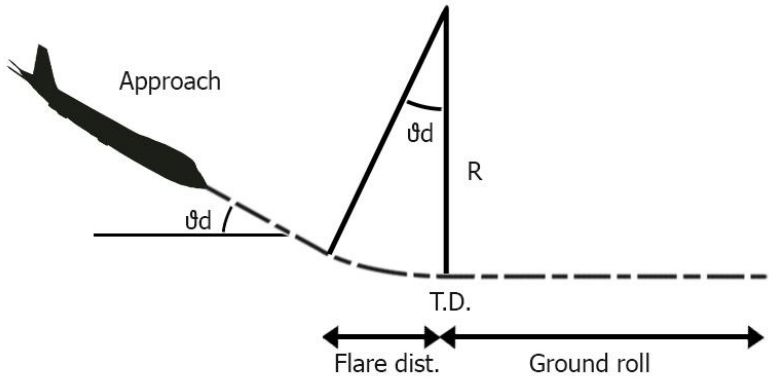

Figure 3-13. Landing diagram

As shown, the landing will be divided into three stages:

1) Approach: a stabilized descent.
2) Flare: the final pull-up before contact to the ground.
3) Free roll and breaking: arresting the horizontal momentum mainly through friction.

3.6.1 Approach

It will be assumed an asymptotic velocity for the descent close to the stall speed so that the aircraft momentum will be very limited by the time it will meet the runway.

This analysis aims to calculate the angle of descent (ϑd) while considering the descent stabilized (without acceleration).

$$D = T + W \cdot \sin\vartheta_d \;\rightarrow_{low\ \vartheta_d}\; \sin\vartheta_d = \frac{1}{E} - \frac{T}{W}$$

In order to calculate the efficiency, we need to evaluate both the coefficient of lift and drag.

$$V_{descent} = 1.3 \cdot V_{stall} = 3.91\ {}^{m}/_{S} \quad \rightarrow \quad C_{L_{descent}} = \frac{C_{L_{maxLanding}}}{(1.3)^2} = 1.065$$

($C_{L_{maxLanding}}$) Lift Coefficient in landing configuration, with flaps fully extended and landing gear deployed. $C_{L_{maxLanding}} = 1.8$

While calculating the drag coefficient, it must be considered the added drag from the extended flap and landing gear, in the form of an additional zero-lift drag coefficient (ΔC_{D0_lift}).

$$C_{D_{Landing}} = C_{D_0} + \Delta C_{D_{0\_Landing}} + \frac{C_{L_{descent}}^{\ 2}}{\pi \cdot AR \cdot e} \cdot K_{GE} = 0.045 + 0.05 + \frac{C_{L_{descent}}^{\ 2}}{\pi \cdot AR \cdot e} \cdot K_{GE} = 0.146$$

(e) Oswald efficiency number. $e = 0.85$

(K_{GE}) Ground Effect modifier. $K_{GE} = 0.9$

It is now possible, after some consideration regarding the thrust, that will be kept minimal during the descent, to calculate the ϑd.

$$E = \frac{C_{L_{descent}}}{C_{D_{Landing}}} = 7.30 \qquad \rightarrow \ \vartheta_d = 5.00\ deg$$
$$T = \varphi \cdot T_0 = 0.05 \cdot 30 = 1.49\ N$$

3.6.2 Flare

Beginning from the flare, to not overshoot the runway, the horizontal distance covered by the aircraft will be taken into account.

$$S_{flare} = R \cdot \sin \vartheta_d$$

It is possible to calculate the flare radius by assuming the maneuver to be stabilized, through a similar process used for the turning analysis of *Paragraph 3.5*.

To apply the forces equilibrium equation, two assumptions are made regarding the flare load factor and the flare velocity, which will be considered as the average between the $V_{descent}$ and the velocity at Touch-Down (V_{TD}).

$$V_{flare} = \frac{V_{descent} + V_{TD}}{2} = \frac{1.3 \cdot V_{stall} + 1.15 \cdot V_{stall}}{2} = 3.69\ {}^{m}/_{S}$$
$$n_{flare} = 1.2$$

$$R = \frac{{V_{flare}}^2}{g \cdot (n_{flare} - 1)} = 6.99\ m$$

It can now be calculated the horizontal space needed for the flare.

$$S_{flare} = R \cdot \sin \vartheta_d = 0.61\ m$$

3.6.3 Ground Roll

The final stage of the landing is divided into two phases:

- The Free Roll: it covers the first 2 seconds of the Ground Roll when typically, the lift is still great enough that is possible to not consider the friction coming from the interaction between the wheels and the runway.
- Ground Roll: the deceleration phase, that, for this aircraft, being unequipped of brakes or thrust reversers, will be determined by aerodynamic drag and friction drag from the wheels.

As shown in the previous paragraph, the velocity of the aircraft at Touch-Down is known. That information allows to easily calculate the Free Roll horizontal distance:

$$S_{FreeRoll} = V_{TD} \cdot \Delta t_{FreeRoll} = 1.15 \cdot V_{stall} \cdot \Delta t_{FreeRoll} = 6.92\ m$$

Assuming two seconds of Free Roll ($\Delta t_{FreeRoll} = 2\ s$).

Ultimately, it must be assessed the distance covered during the Ground Roll. The main parameter that will influence it will be the deceleration coming from both aerodynamic drag and rolling friction.

Conveniently, both those forces are essentially constant for most of the landing, allowing simplifying the analysis and estimating them at a fixed velocity.

$$V_{GR} = 0.7 \cdot V_{TD} = 2.42\ {}^{m}/_{s}$$

$$a_{GR} = \frac{[D + \mu_r (W - L)]_{V=0.7V_{TD}}}{{}^{W}/_{g}} = -0.288\ {}^{m}/_{s^2}$$

(a_{GR}) Ground Roll acceleration.

(μ_r) Rolling friction coefficient. $\mu_r = 0.025$

By construction, when the landing gear is in contact with the ground, the angle of attack of the wing will be close to 0 degrees. That allows estimating the value of the Coefficient of lift and, consequentially the Coefficient of Drag, which will also contain the information regarding the zero-lift drag coefficient given by the landing gear and flaps.

$$C_{L_{GroundRoll}} = 1.1$$

$$C_{D_{GroundRoll}} = C_{D_0} + \Delta C_{D_{0\_Landing}} + \frac{{C_{L_{GroundRoll}}}^2}{\pi \cdot AR \cdot e} * K_{GE} = 0.149$$

Final results:

Aerodynamic Drag	0.159	[N]
Rolling friction Drag	0.719	[N]
Mean acceleration	-0.288	[m/s^2]

Table 3-5. Mean braking forces during Ground Roll

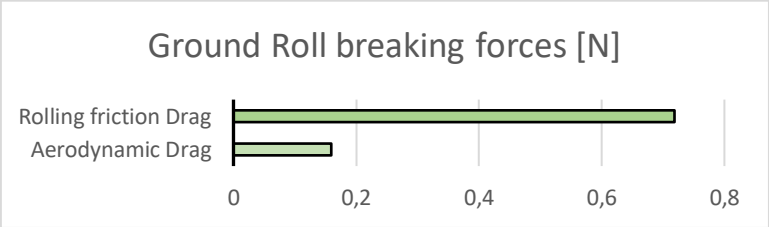

Figure 3-14. Mean braking forces during Ground Roll

Ground Roll horizontal distance (S_{GR}):

$$S_{GR} = \int_0^{V_{TD}} \frac{dV^2}{2 \cdot a_{GR}} = \frac{{V_{TD}}^2}{2 \cdot a_{GR}} = 20.81\ m$$

Total landing distance:

$$S_{Landing} = S_{flare} + S_{FreeRoll} + S_{GR} = 28.34\ m$$

4 Bibliography

[1] John D. Anderson, “Aircraft performance and design”, McGraw-Hill International Editions Series, 1999.

[2] Egbert Torenbeek; H. Wittenberg, «Flight Physics: Essentials of Aeronautical Disciplines and Technology», Springer, 2009.

[3] Jan Roskam, «Airplane Flight Dynamics and Automatic Flight Controls», DARcorporation, 2001.

[4] «Flight Testing Newton's Laws Instructor's Flight Manual», Dryden Flight Research Center, NASA.

[5] Robert T. Marshall, Flight Research Center NASA, «Flight-Determined Acceleration and Climb Performance of an F-104G Airplane for use in an Optimum-Flight-Path Computer Program», 1971.

[6] Nancy Hall, NASA,«Glide Angle and Glide Ratio» (https://www.grc.nasa.gov/www/k-12/airplane/glidang.html), 2021.

[7] Agostino De Marco, Domenico P. Coiro, Fabrizio Nicolosi, «Elementi di Meccanica del Volo», 2017.

[8] Shreyas S Hegde, Sandeep Nayak, Kishan R, Narayan Chavan, Department of Mechanical Engineering of NITK Surathkal, «A Systematic Approach for Designing, Analyzing and Building a Model RC Plane», 2014.

[9] Scott Blackwelder, «UAV Flight Dynamics», International Journal of Aeronautical Science & Aerospace Research (IJASAR), 2015, ISSN: 2470-4415.

[10] Kadir Alpaslan Demir, Halil Cicibas, and Naz Arica, «Unmanned Aerial Vehicle Domain: Areas of Research», Defence Science Journal, Vol. 65, No. 4, July 2015.

[11] Gavin Ananda, «UIUC Propeller Database – Volume 1», University of Illinois Urbana-Champaign.

[12] Rafi ur Rahman, Muhammed Hasnain Kabir Nayeem, Mosarruf Hossain, Md. Roman Hossain Fazlah Rabby, «Design and performance analysis of unmanned aerial vehicle (UAV) to deliver aid to the remote area», International Conference on Mechanical, Industrial and Materials Engineering 2017, Paper ID: RT-207.

Un caloroso ringraziamento a tutte le persone che mi sono state accanto durante il mio percorso di laurea, e a tutti coloro che mi sono stati maestri, sia in ambito accademico, che nel quotidiano.

Ringrazio la mia famiglia, mio padre, mia madre e mio fratello per il costante supporto e incoraggiamento, nonchè per tutto ciò che mi hanno trasmesso.

Un sentito ringraziamento al mio relatore, Danilo Ciliberti, il quale è riuscito sempre a trasmettere la passione che lo contraddistingue nel corso di questo progetto, rendendosi disponibile per chiarire ogni dubbio.

Ringrazio inolte il Professor Fabrizio Nicolosi che per primo mi ha introdotto alla materia trattata, le cui lezioni cariche di entusiasmo non dimentichero mai.

Un dovuto ringraziamento a Marco, Francesco, Francesco e Francesco, che hanno creduto in questo progetto, arrivando alla stesura di una serie di documenti che ci hanno reso fieri delle conoscenze acquisite in questi anni.

Concludo ringraziando nello specifico tutti i colleghi e ormai amici a vita dell'associazione «EUROAVIA NAPOLI Umberto Nobile», che sono stati modelli di riferimento, innescando in me una crescita personale e professionale che mi accompagnerà per tutto il resto della mia carriera.